### Title

On statistical Multi-Objective optimization of sensor networks and optimal detector derivation for structural health monitoring




### Authors

Colombo, Luca
Todd, MD
Sbarufatti, C
et al.



### Publication Date

2022-03-01

### DOI

10.1016/j.ymssp.2021.108528

Peer reviewed

# On Statistical Multi-Objective Optimization of Sensor Networks and Optimal Detector Derivation for Structural Health Monitoring

L. Colombo, M. D. Todd, C. Sbarufatti, M. Giglio

Politecnico di Milano, Dept. of Mechanical Engineering, via La Masa 1, 20156 Milano, Italy, luca1.colombo@polimi.it

University of California, Dept. of Structural Engineering, 9500 Gilman Drive, La Jolla, San Diego, CA 92093-0085, United States, mdtodd@eng.ucsd.edu

Politecnico di Milano, Dept. of Mechanical Engineering., via La Masa 1, 20156 Milano, Italy, claudio.sbarufatti@polimi.it

Politecnico di Milano, Dept. of Mechanical Engineering., via La Masa 1, 20156 Milano, Italy, marco.giglio@polimi.it

**Keywords:** optimal sensor placement; optimal detector; Bayes cost; classification; Neyman-Pearson; multi-objective optimization.

## Abstract

Sensor placement and structural health classifiers are fundamental components of Structural Health Monitoring (SHM) systems, as they largely define system detection (or classification) performance. Optimal sensor placement strategies are designed to maximize the ability to detect damage or to minimize lifetime costs, given limited resource availability. However, usually choosing one strategy over the other and non-optimal detector implementation may provide poorly performing solutions in terms of detection performance or total cost, even though both are critical objectives for a cost-effective SHM system implementation.

The work proposes a unique and coherent framework for optimal detector and sensing network design for SHM. After an optimal detector is defined based on the Neyman-Pearson likelihood ratio test, classification performance indexes are used in a multi-objective optimization paradigm for optimal sensor placement. Specifically, the optimization considers maximizing the classification performances and, simultaneously, minimizing a measure of total cost or risk in a Bayesian sense.

Even though the approach is general for any structure and sensor measurement process, the method is numerically verified with a cracked plate under tension and monitored by measurements of local strain serving as the surrogate SHM system. The results are also validated by comparing the multi-objective optimal design to engineering judgment and single-objective-based solutions in terms of probability of detection and costs. The advantages of an optimization scheme are emphasized with respect to an engineering scheme and, above all, how a *multi-objective optimization strategy* reflects a conjunct saving in costs and improvement in detection performances.

## Nomenclature

| | |
|---|---|
| $A$ | Damage-sensitive feature in the actual condition |
| $B$ | Damage-sensitive feature in the baseline condition |
| $X$ | Difference between the actual and baseline features |
| $i, W$ | Damage index |
| $H_0$ | Undamaged condition |

| | |
|---|---|
| $H_1$ | Damaged condition |
| $\mu_X$ | Mean of $X$ |
| $\sigma_X^2$ | Variance of $X$ |
| $f_W$ | The probability density function of the damage index in the undamaged scenario |
| $f_{W_d}$ | The probability density function of the damage index in the damaged scenario |
| $N$ | Number of data samples |
| $D$ | Optimal detector |
| $\gamma'$ | The threshold for health classification |
| $P_{FA}$ | Probability of false alarms |
| $P_D$ | Probability of detection |
| $C_B$ | Bayes cost |
| $L$ | Neyman-Pearson likelihood ratio |
| $p(D, H_i)$ | The probability density function of the detector under $H_i$ |
| $P_{FA_{MC}}$ | Probability of false alarms computed with Monte Carlo |
| $N_{MC}, N_{MC_1}$ | Number of Monte Carlo samples |
| $P_e$ | Probability of making an error |
| $R$ | Risk/cost function |
| $x_{t_i}$ | Sensor position |
| $P_{D_{sys}}$ | Probability of detection of the SHM system |
| $\Omega$ | Structure's domain |
| $S_k$ | Set of detectors associated with the sensors in region $k$ |
| $C_s$ | Cost of the system |
| $C_{00}$ | Cost of true negatives |
| $C_{10}$ | Cost of false positives |
| $C_{01}$ | Cost of false negatives |
| $C_{11}$ | Cost of true positives |
| $n_r$ | Number of regions |
| $P(H_{i,k})$ | Probability of region $k$ of being in the state $H_i$ |
| $P_{FA_B}, P_{D_B}$ | Probability of false alarms/detection for the Bayes risk |
| $P(H_1)$ | The total probability of a damaged state |
| $P(H_0)$ | The total probability of an undamaged state |
| $d_{\text{opt}}$ | Optimal design |
| $\alpha$ | Weight parameter governing the relative importance of the two objective functions |
| $y_1$ | Value of the first objective function |
| $y_2$ | Value of the second objective function |
| $CtoC$ | Classification improvement to cost increase ratio |

## 1. Introduction

In recent years, structural integrity demands have driven scientific and industrial communities' research into developing a framework for informing structural diagnostics, generally known as Structural Health Monitoring (SHM). SHM aims at real-time, automatic evaluations of the structures' health conditions based on a network of permanently installed sensors [1]–[5], leading to the expectation of considerable operative cost reduction and improved safety margins. This is because SHM may then be used to inform predictive models about future structural performance in order to accomplish optimal maintenance, limit state (e.g., failure) prediction, or other goals, potentially resulting in total life cycle cost savings.

Sensor network design, including the number and location of sensors, is among fundamental steps of SHM system development, part of "operational evaluation" in the modern SHM paradigm where the target damage, design and environmental constraints, and other parts of the problem are defined as well as possible

[6]–[9]. With such things defined, *in-situ* measures of structural response (“raw data”) are collected from a given sensor network design from which *features* are extracted. These features then become the information by which damage assessment is accomplished by comparing a baseline set representative of the undamaged structure and a test set; this baseline set is obtained either by direct measurements in the baseline condition (a baseline “database”) or by modeling assumptions, such as linearity [10] or correlation between sensor pairs [11]. These features usually assume the form of direct waveform metrics, data- or physics-based model parameters, or residual model errors. Finally, the features are then modeled under statistical hypothesis testing procedures to assess damage presence, location, and/or severity [6], [12]. This particular statistical modeling step can take several forms, and as will be discussed later, it may be accomplished optimally by deriving a *detector* that is appropriate for the hypothesis test(s) being considered.

It is clear, then, that design factors in the initial sensor network may influence the ultimate performance efficiency of the classifying scheme regardless of whether it is optimal or not. As such, several previous works in the literature consider distributed sensor network design for SHM applications, using, e.g., strain measurements [13] or piezoelectric-based measurements [14]–[17]. Some works [18], [19] minimize the norm (trace or determinant) of the Fisher information matrix computed from the modal and measurement covariance matrixes. Others [20]–[24] define sensor networks based on the concept of observability, or the network’s ability to infer the state parameters required for performance monitoring, health assessment, and system control. The information may be provided by directly measuring the system parameters or reconstructing unobservable system parameters based on observable ones. Methods based on fault diagnosis [25]–[28] extend the observability analysis with state variables, and their response are indicative of health conditions. The performance metric defines the sensing network’s ability to distinguish fault conditions from nominal operation (fault detection) and, possibly, discern among the different faults (fault discrimination).

Thus far, sensor network design for SHM has been mostly driven by maximizing some aspect of feature discrimination (through many forms, as indicated above), or, more directly, by maximizing the likelihood that target damage is detected [29]. Recently, in [15], [30]–[35], optimal sensor placement strategies for SHM were proposed in various forms of a Bayesian formulation accounting for the distributed cost of type I (false positive) and II (false negative) decision errors, which sought to minimize the lifetime cost, defined by a Bayes risk metric. These two overall objective schemes--maximizing the probability of detection/classification and minimizing costly errors (generalized to all incurred monitoring costs)--comprise two (potentially) competing goals; it is not clear what favoring one strategy does when evaluated by the other strategy’s objective in terms of design consequences. Both strategies are fundamental aspects of any successful but cost-effective SHM system. The specific SHM application is typically the driver, where applications demanding life-safety consideration might favor maximum classification/detection performance design (e.g., commercial airframe inspections), while applications requiring minimized downtime (e.g., a manufacturing process) might favor a minimal risk/cost design. The majority of SHM applications, one could argue, demand some combination of detection performance and cost minimization, and this paper is a consideration of both objectives simultaneously. To the best of the authors’ knowledge, no SHM studies so far have considered such multi-objective optimal sensor design.

As part of the ultimate goal of formulating and exploring the multi-objective SHM sensor optimization problem, this paper employs formal principles of detection theory to design an optimal detector for the general binary damage detection hypothesis test that will be proposed. The use of detection theory [36] ensures a consistent statistical framework in defining the optimization problem; specifically, the detector will be derived by the Neyman-Pearson theorem, which invokes a probabilistic likelihood ratio test that optimizes the hypothesis selection for deciding whether damage is present or not. Other detectors could be derived (e.g., a minimal probability of error detector), but any detector could be used to formulate the bigger SHM design optimization problem [36]. The specific performance of which optimal detector to use is not within

the scope of this present paper. It will be left to future work to consider a fully coupled sensor design optimization strategy where the detector design itself is part of that global optimization. Thus, in this work, once the optimal Neyman-Pearson detector is defined, the multi-objective SHM design objective will be formulated, and the relative importance of a minimum cost strategy compared to maximum detection/classification strategy is analyzed in detail, providing insights into the consequences in terms of costs and probability of detection when choosing one strategy over another. Specifically, the proposed optimal sensor placement strategy combines maximum classification performance and minimum cost of the system, including costs associated with wrong decisions.

The paper undertakes this formulation in a simple case study constituted by a clamped plate under tension and damaged with cracks. An SHM system with a strain-based data collection system is considered for demonstrating the method and consequences of choosing one optimization strategy over the other in terms of costs and detection probability. The optimization is performed based on a genetic algorithm [37], [38] for its widely recognized robustness. Different sensitivity analyses have been performed, including but not limited to, comparison between optimal designs obtained with the proposed multi-objective framework and the classical single-objective optimization, providing insight into the method's advantages in terms of structured design decisions. The Receiver Operating Condition (ROC) curve is also provided as a performance indicator of different designs. The simplicity of this SHM application example is designed in order to evaluate the multi-objective considerations without obfuscation from challenges that might arise from a more complex (and admittedly, more realistic) SHM application.

The paper is structured as follows. The design of the optimal detector is provided in Section 2, and it is used for subsequent presentation of the multi-objective paradigm for optimal sensor placement in Section 3. Section 4 provides information on the application case for sensing network optimization, while results are shown in Section 5 for the test cases under varying problem boundary conditions and comparison scenarios. A conclusion section completes the paper.

## 2. Definition of an optimal statistical detector

A detector may be informally thought of as the transformation from feature to decision. In this work, only binary decisions will be considered (rather than a generalized regression into multiple data classes), where one typically must decide whether features obtained from a test belong to the reference ("baseline") condition or not ("damaged"). One of the most common metrics used to quantify this is the squared difference $i(t)$ between them, or

$$i(t) = (A(t) - B)^2 = X(t)^2 \quad \text{with} \quad X(t) = A(t) - B, \tag{1}$$

where $A(t)$ and $B$ are the features in the test and baseline conditions, respectively. It is noted that this is only one possible metric of difference, as many other types of metrics could be formulated, leading to different subsequent specific optimal detector mathematical transformations. However, the methodology that follows below may be applied to any such metric, and this paper considers the squared difference metric because it is among the most common used for features that, generally speaking, can be both positive and negative in value (such as a strain measurement, as in the application in this work).

The detection of damage is then transformed into a binary decision between choosing the undamaged condition (implying $i(t) = 0$), or the damage condition (implying $i(t) \neq 0$). However, statistical variability in the features may cause the index to deviate from zero even in the undamaged scenario. Detection theory provides a methodology for deriving optimal detectors (for classifying any metric or feature, such as in Eq. (1), to guarantee that robust decisions can be performed in realistic scenarios. An optimal detector's construction procedure leverages a likelihood ratio test under a binary hypothesis formulation: undamaged, $H_0$ $(i = 0)$, and damaged, $H_1(i \neq 0)$, states. A likelihood ratio test corresponding to a binary hypothesis

guarantees that the resulting detector is optimal [39], in the sense that it uniformly represents the most powerful test among the alternative tests.

One type of detector optimality in this context is to minimize the probability of choosing $H_0$ when $H_1$ is actually true, $p(H_0; H_1)$, or equivalently, to maximize the probability of choosing $H_1$ when $H_1$ is actually true, $p(H_1; H_1)$. The probability of choosing $H_1$ when $H_1$ is actually true corresponds to the probability of detection, $P_D$, and this strategy comprises the Neyman-Pearson approach [36], [39]. Another type of optimality strategy is to minimize decision errors, e.g., the probability of choosing $H_0$ conditioned upon $H_1$ being observed as the result of a probabilistic test, $p(H_0|H_1)$, and/or the complementary decision error, $p(H_1|H_0)$. There is a subtle but important notational difference in the probabilities using a semi-colon (;) and a vertical line (|). The former notation, e.g., $p(H_i; H_j)$, describes the probability of choosing $H_i$ when $H_j$ is true without any probabilistic meaning assigned to the likelihood that $H_j$ is true. The latter notation, e.g., $p(H_i|H_j)$, describes the probability of choosing $H_i$ conditioned upon a probabilistic test that indicated $H_j$ is true, i.e., $p(H_j)$, which is typically based on assumptions, prior knowledge, previous tests, etc. The law of conditional probabilities may be then used to define the total probability of making a decision error, $P_e$, in a way consistent with Bayesian reasoning. As mentioned, this work will select the Neyman-Pearson optimality criterion for detector design, but the minimum error detector (or other designs) could be considered.

Regardless of the optimality strategy, of course, a statistical model for the hypothesis test must be formed, and the Neyman-Pearson detector design will now be considered. Using the central limit theorem, it is first assumed that $X$ may be modeled as normally distributed with variance, $\sigma_X^2$, and that damage produces a change in the mean of *X*, $\mu_X$, without a change in variance. The formal hypothesis test may be formally stated as

$$H_0: X \sim N(0, \sigma_X^2) \tag{2}$$

and

$$H_1: X \sim N(\mu_X, \sigma_X^2). \tag{3}$$

Let us next recall the damage index metric, $i = X^2 = W$. Using the probability transformation theorem and some mathematical manipulation, the probability distributions of *W*={*w[0]*} for a single observation of the damage index under the two hypotheses may be written as

$$p(w[0]; H_0) = f_W = \frac{1}{\sigma_X}\frac{1}{\sqrt{2\pi}} w[0]^{-\frac{1}{2}} e^{-\frac{w[0]}{2\sigma_X^2}} \tag{4}$$

and

$$p(w[0]; H_1) = f_{W_d} = \frac{e^{-\frac{1}{2}\left(\frac{w[0]+\mu_X^2}{\sigma_X^2}\right)} \cosh\left(\frac{\mu_X}{\sigma_X^2}\sqrt{w[0]}\right)}{\sqrt{2\pi w[0]}\sigma_X} \tag{5}$$

In real applications, one is likely to compute more than a single feature over time, leading to many observations of the damage index metric. Supposing that $N$ such metrics are independently collected, *W*={*w[k]*, *k*=1…*N*}, the probability density functions (pdfs) of Eqs. (4) and (5) further transform to

$$f_W = e^{-\frac{1}{2\sigma_X^2}\sum_{k=1}^{N} w[k]} \prod_{k=1}^{N} \frac{1}{\sigma_X}\frac{1}{\sqrt{2\pi}} w[k]^{-\frac{1}{2}} \tag{6}$$

and

$$f_{W_d} = e^{-\frac{1}{2\sigma_X^2}\sum_{k=1}^{N}(w[k]+\mu_X^2)} \prod_{k=1}^{N} \frac{1}{\sqrt{2\pi w[k]}\sigma_X} \cosh\left(\frac{\mu_X}{\sigma_X}\sqrt{w[k]}\right) \tag{7}$$

The two parameters $\mu_X$ and $\sigma_X$ may be estimated from $X$ using a Maximum Likelihood Estimate (MLE) approach [40]. Given the pdf of *X*, the Generalized Likelihood Ratio Test (GLRT) requires computing the MLE of the unknown parameters

$$\begin{bmatrix}\mu_X \\ \sigma_X\end{bmatrix} = \overline{\boldsymbol{\Theta}_\iota} = \mathrm{argmax}_{\Theta_\mathrm{i}}\big(p(X; \boldsymbol{\Theta}_\mathrm{i}, H_i)\big), \tag{8}$$

where the latter is found by taking the gradient of the pdf and setting it to zero

$$\overline{\boldsymbol{\Theta}_\iota} = \frac{\partial p(X; \boldsymbol{\Theta}_\mathrm{i}, H_i)}{\partial \boldsymbol{\Theta}_i} = \mathbf{0}. \tag{9}$$

Considering the pdf of $X = \{x[k], k = 1 \dots N\}$ under $H_1$ as

$$p_X(x[k]; H_1) = \frac{1}{(2\pi\sigma_X^2)^{\frac{N}{2}}} e^{-\frac{1}{2\sigma_X^2}\sum_{k=1}^{N}(x[k]-\mu_X)^2}, \tag{10}$$

taking the partial derivatives with respect to $\mu_X$ and $\sigma_X$ results in the MLEs of the parameters:

$$\begin{aligned} \mu_X &= \frac{1}{N}\sum_{k=1}^{N} x[k] \\ \sigma_X &= \sqrt{\frac{1}{N}\sum_{k=1}^{N}(x[k]-\mu_X)^2}\,. \end{aligned} \tag{11}$$

With these parameters now estimated, the Neyman-Pearson optimal likelihood ratio test is computed as

$$L(w[k]) = \frac{f_{W_d}}{f_W} > \gamma, \tag{12}$$

where $\gamma$ is a threshold for the hypothesis selection decision (defined shortly). Substituting the expressions of $f_W$ and $f_{W_d}$ and taking the logarithm of both sides (which doesn't affect the detector, since the logarithm is a monotonic function), the optimal Neyman-Pearson detector, $D$, is finally obtained as

$$D = \ln\big(L(w[k])\big) = -\frac{N\mu_X^2}{2\sigma_X^2} + \sum_{k=1}^{N} \cosh\left(\frac{\mu_X}{\sigma_X^2}\sqrt{w[k]}\right) > \ln(\gamma) = \gamma'. \tag{13}$$

Under the Neyman-Pearson theorem, this detector *D* will maximize the probability of detection, $P_D$, given by

$$P_D = \int_{\gamma'}^{\infty} p(D; H_1) dD, \tag{14}$$

where $p(D; H_1)$ is the distribution of the detector $D$ under $H_1$. A detection test is performed by comparing the value of the detector $D$ with the threshold, $\gamma'$. Detector values $D$ that exceed the threshold $\gamma'$ imply choosing $H_1$ ("damage condition") is the right decision, while values that don't exceed the threshold $\gamma'$ imply choosing $H_0$ ("baseline condition") is the right decision. This threshold $\gamma'$ is determined by the (application-dependent) allowable probability of false positives ("false alarms"), $P_{FA}$, defined by

$$P_{FA} = \int_{\gamma'}^{\infty} p(D; H_0) dD, \tag{15}$$

where $p(D;H_0)$ is the distribution of the detector under $H_0$. Eqs. (14) and (15) often cannot be solved analytically in closed form and must be solved numerically. Such is the case in this work, as the transformation from $p(w[k])$ to $p(D)$ indicated by Eq. (13) is not analytically tractable.

An example of the numerical procedure based on Monte Carlo simulations is utilized hereafter. Given a probability of false alarm level chosen according to the specific problem, the threshold for each test sensor, $\gamma'_{MC}$, can be obtained minimizing an error functional defined comparing $P_{FA}$ with the numerically computed version of the same, $P_{FA_{MC}}$, through Monte Carlo:

$$\gamma'_{MC} = \mathrm{argmin}_{\gamma}\left(\ln\left(\left(\mathrm{P_{FA}} - \mathrm{P_{FA_{MC}}}(\gamma)\right)^2\right)\right). \tag{16}$$

The probability of false alarm as a function of the threshold can be computed according to the pseudocode below:

for ii=1:$N_{MC}$

for jj=1:$N_{MC_1}$

- extract $N$ random normal samples with zero mean and $\sigma_X^2$ variance
- estimate the mean and variance
- compute the detector *D*
- aggregate all realizations of the detector

end

- Count the number of times the sampled detectors exceed the threshold considered
- Divide the number by $N_{MC_1}$
- Collect the results

end

- Average the results

In the previous, $N_{MC}$ and $N_{MC_1}$ are the number of Monte Carlo samples and need to be sufficiently high to produce a small error in the estimated quantities. Once the threshold is computed as a function of the probability of false alarms, the detector of Eq. (13) is completely defined and can be implemented for damage detection.

Just as with calculating $P_{FA}$, a Monte Carlo numerical procedure can be followed for calculating $P_D$. The pseudocode for computing the probability of detection for each sensor as a function of damage is reported below:

For kk=1:$N_{\mathrm{damages}}$

for ii=1:$N_{MC}$

for jj=1:$N_{MC_1}$

- extract $N$ random normal samples with mean $\mu_X$ and variance $\sigma_X^2$
- estimate the mean and variance
- compute the detector D
- collect the detector

end

- Count the number of times the sampled detectors exceed the threshold
- Divide the number by $N_{MC_1}$
- Collect the results

end

- Average the results

end

Even though this Neyman-Pearson detector will be used going forward in formulating the optimal design problem, it is worth briefly presenting another common detector approach, primarily because its formulation mirrors the formulation of the larger minimum risk/cost optimization problem. Recall the second detector optimality criterion considered minimizing decision errors, which may be even further generalized to minimizing the costs associated with those decision errors. As mentioned prior to Eq. (2), the law of total conditional probability may be used to arrive at the total probability of making an error, $P_e$, given in the binary case by

$$P_e = P(H_0|H_1)P(H_1) + P(H_1|H_0)P(H_0). \tag{17}$$

This can be mapped into a cost function *R* by assigning a cost $C_{ij}$ to each decision, both the incorrect decisions given by $P_e$ as well as the correct decisions such that

$$R = \sum_{i,j=0}^{1} C_{ij} P\left(H_i \middle| H_j\right) P\left(H_j\right). \tag{18}$$

The costs $C_{ij}$ serve as weights on various decision probabilities (both correct and incorrect), and the function *R* is minimized [36] according to a similar likelihood ratio test (analogous to the Neyman-Pearson likelihood test) given by

$$L(w[k]) = \frac{p(w[k]|H_1)}{p(w[k]|H_0)} > \gamma = \frac{(C_{10} - C_{00})P(H_0)}{(C_{01} - C_{11})P(H_1)}, \tag{19}$$

where the threshold is now determined by prior knowledge and decision consequence costs. Thus, this minimum risk detector establishes a decision rule that minimizes the total cost of making all decisions, rather than a decision rule that maximizes the probability of making the correct "true positive" decision (i.e., the probability of detection).

## 3. The sensor network optimization procedure

The use of an (optimal) detector ensures a statistically rigorous transformation from feature space to decision space. With such a decision rule in place, it is generally true that the specific sensor network design used could influence the performance of the decision rule. In the simplest case, for example, it is entirely reasonable to assume that sensors placed in low signal-to-noise ratio locations, or perhaps rather insufficient observability of the network, would affect the overall SHM system's performance, as quantified by some global metric. As discussed in Section 1, SHM sensor network optimization, broadly defined, follows two potential objectives: (1) maximizing some measure of feature discrimination, generally meaning maximizing the system's global probability of detection $P_D$, or (2) minimizing the total decision and operational cost of the SHM system, generally meaning minimizing the consequence costs of all decisions the SHM is asked to make together with what the cost of the particular SHM system deployment is. It is worth noting that both of these broad objectives mimic the optimal detector decision rules derived in Section 2. In Section 3.1, the Neyman-Pearson detector rule is generalized for a sensor location under multiple possible damage locations and then fused into a global measure of $P_D$ for any particular sensor location. The multi-objective

optimization problem is then defined in Section 3.3, providing the fitness functions to maximize the probability of detection and minimize the total cost (defined as a Bayes risk measure), which are aggregated into a single weighted objective function.

### 3.1 Extension to multiple sensors and possible damage locations

The probability of detection for the single sensor defined in Section 2 can be first defined for the more general case of detecting damage that is located at different locations on the structure. Considering damage occurrences to be independent in space, i.e., the probability of the sensor detecting damage at one location is independent of its probability to detect damage at another location, the total probability of detection for that single sensor (located at position $x_{t_i}$) is

$$P_D(x_{t_i}) = \prod_{i=1}^{N_{\text{damages}}} P_{D_i}. \tag{20}$$

Eq. (20) applies only to a single-sensor design, and this definition must be modified to account for the more typical problem of using a network of such sensors. This is fundamentally a problem in sensor fusion, which can occur at many levels of the "data to decision" process [41]. In this work, a single vote fusion rule is used, where global detection is achieved if any one of the detectors computed at each of the $x_{t_i}$ sensor positions exceeds its local Neyman-Pearson threshold $\gamma_i$. A schematic workflow of this fusion rule is provided in Fig. 1.

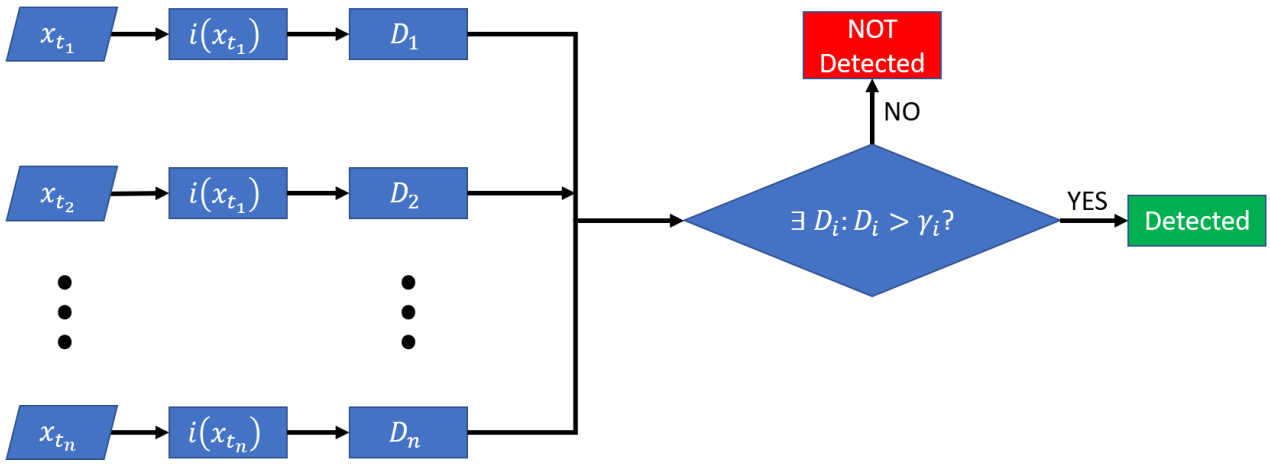


**Fig. 1. Sensor fusion rule for defining the detection of a true positive.**

With a true positive detection thus defined, the global probability of detection would require running Monte Carlo simulations over the entire sensor network design space, leading to a demanding computational procedure for an optimization framework. Sequential block simplification overcomes the need for a Monte Carlo simulation. The probability of detection can be computed only once, for each test sensor position available, according to Eq. (20), and the system probability of detection can be calculated from the $P_{D_i}$ of the sensors that comprise the network. Fig. 2 shows the working principle of sequential block simplification with a generic sensor network composed of $n$ sensors with probability of detections $P_{D_i}$ $(i = 1, \dots, n)$. The algorithm considers a random pair of sensors ($i$ and $i+1$) and substitutes their individual probability of detections with an equivalent probability of detection, $P_{D_{i-i+1}}$, until the entire sensor network is systematically analyzed. The equivalent joint probability of detection for a pair of sensors, $i$ and $i+1$, is defined as

$$P_{D_{i-i+1}} = P_{D_i} + P_{D_{i+1}} - P_{D_i} P_{D_{i+1}}. \tag{21}$$

Thus, a computationally efficient formulation of the system's global probability of detection can be derived and implemented in an optimization framework shown in Fig. 2.

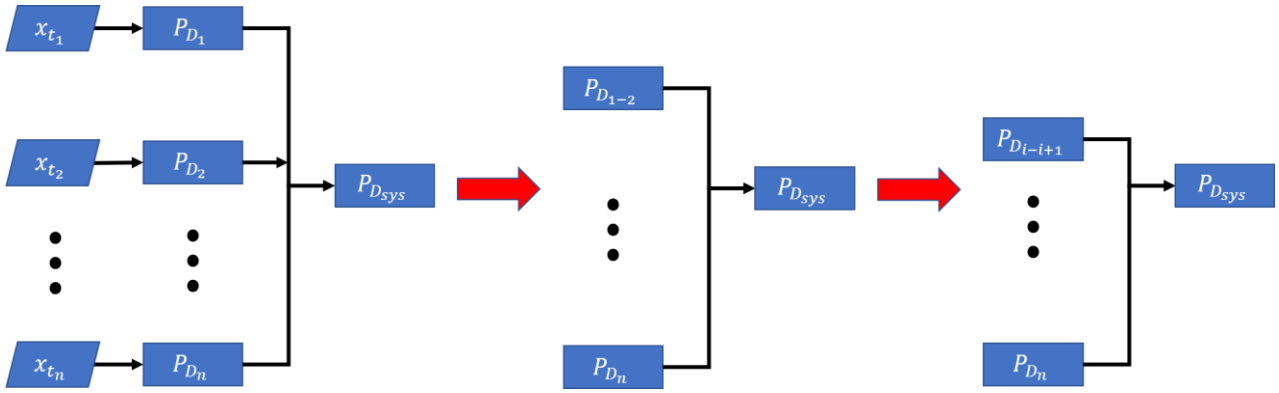


**Fig. 2. Sequential block simplification workflow.**

### 3.2 Definition of the Bayes risk/cost

For scenarios where the probability of possible outcomes is established a priori, Bayes risk is a popular decision-making optimality criterion. As introduced in Eq. (18), $R$ is the sum of each outcome's expected cost, defined as the cost of each event multiplied by its probability; in SHM, they consist of all the possible combinations of the structure's predicted and true damage states. Expanding on the previous definition of the Bayes risk, the desired practical form is derived. The latter can be implemented in a multi-objective optimization strategy that will be the focus of Section 3.3.

In this work, the damage state is considered as a simple binary condition: either damaged or undamaged. Furthermore, considering that the cost and probabilities can vary continuously within the structure domain $\Omega \in \mathbb{R}^3$, the global risk metric is derived as

$$R = \int_{\Omega} \sum_{i,j=0}^{1} C_{ij} P(H_i|H_j) P(H_j) \tag{22}$$

Operatively, Eq. (22) can be approximated by discretizing the structure in $n_r$ regions small enough to consider the costs and probabilities constant within each region domain, $\Omega_k$, and equal to the integral of their distribution within each region. The risk can then be written as:

$$R = \sum_{k=1}^{n_r} \sum_{i,j=0}^{1} C_{ij,k} P(H_{i,k}|H_{j,k}) P(H_{j,k}) \tag{23}$$

where $\cdot, k$ refers to the risk/cost associated with region $k$. For the sake of simplicity, Eq. (23) is written explicitly as

$$\begin{aligned} R = &\sum_{k=1}^{n_r} C_{00,k} P(H_{0,k}|H_{0,k}) P(H_{0,k}) + \sum_{k=1}^{n_r} C_{01,k} P(H_{0,k}|H_{1,k}) P(H_{1,k}) \\ &+ \sum_{k=1}^{n_r} C_{10,k} P(H_{1,k}|H_{0,k}) P(H_{0,k}) + \sum_{k=1}^{n_r} C_{11,k} P(H_{1,k}|H_{1,k}) P(H_{1,k}) \end{aligned} \tag{24}$$

The latter includes costs associated with wrong and correct decisions. The local costs represent the complete cost due to structural health classification with respect to normal operation, resulting in application-specific

coefficients. Specifically, each cost parameter in Eq. (24) refers to the following, where the subscript $k$ is omitted for brevity:

- $C_{00}$ is the cost of true negatives, thus the cost of deciding a structure is undamaged when it is really undamaged. It includes costs related to normal operation.
- $C_{10}$ is the cost of false positives, thus the cost of deciding a structure is damaged when it is really undamaged. It considers out-of-service costs, inspection costs, etc.
- $C_{01}$ is the cost of false negatives, thus the cost of deciding a structure is undamaged when it is really damaged. It considers out-of-service costs, life-safety issues, capital loss, or other failure consequence costs.
- $C_{11}$ is the cost of true positives, thus the cost of deciding a structure is damaged when it is really damaged. It considers out-of-service costs, repair or replacement costs, etc.

The conditional probabilities in Eq. (24) may be further simplified as follows:

$$\begin{aligned}
P(H_{1,k}|H_{1,k}) &= P(\exists D_i \in S_k: D_i > \gamma_i | H_{1,k}) = \frac{P(\exists D_i \in S_k: D_i > \gamma_i \cap H_{1,k})}{P(H_{1,k})} = \frac{P_{D,k}}{P(H_{1,k})} \propto P_{D,k} \\
P(H_{1,k}|H_{0,k}) &= P(\exists D_i \in S_k: D_i > \gamma_i | H_{0,k}) = \frac{P(\exists D_i \in S_k: D_i > \gamma_i \cap H_{0,k})}{P(H_{0,k})} = \frac{P_{FA,k}}{P(H_{0,k})} \propto P_{FA,k} \\
P(H_{0,k}|H_{0,k}) &= P(D_i < \gamma_i \ \forall D_i \in S_k | H_{0,k}) = 1 - P(\exists D_i \in S_k: D_i > \gamma_i | H_{0,k}) = 1 - \frac{P_{FA,k}}{P(H_{0,k})} \propto 1 - P_{FA,k} \\
P(H_{0,k}|H_{1,k}) &= P(D_i < \gamma_i \ \forall D_i \in S_k | H_{1,k}) = 1 - P(\exists D_i \in S_k: D_i > \gamma_i | H_{1,k}) = 1 - \frac{P_{D,k}}{P(H_{1,k})} \propto 1 - P_{D,k}
\end{aligned} \tag{25}$$

where $S_k$ is the set of detectors associated with the sensor in $\Omega_k$.

The Bayes Risk is now proportional to

$$\begin{aligned}
R \propto \sum_{k=1}^{n_r} C_{00,k}(1 - P_{FA,k})P(H_{0,k}) + \sum_{k=1}^{n_r} C_{01,k}(1 - P_{D,k})P(H_{1,k}) + \sum_{k=1}^{n_r} C_{10,k}P_{FA,k}P(H_{0,k}) \\
+ \sum_{k=1}^{n_r} C_{11,k}P_{D,k}P(H_{1,k})
\end{aligned} \tag{26}$$

Considering the cost coefficients constant for all the $n_r$ regions and independent of the various detection probabilities, they may be brought out of the summation to yield

$$\begin{aligned}
R \propto C_{00} \sum_{k=1}^{n_r} (1 - P_{FA,k})P(H_{0,k}) + C_{01} \sum_{k=1}^{n_r} (1 - P_{D,k})P(H_{1,k}) + C_{10} \sum_{k=1}^{n_r} P_{FA,k}P(H_{0,k}) \\
+ C_{11} \sum_{k=1}^{n_r} P_{D,k}P(H_{1,k})
\end{aligned} \tag{27}$$

By applying the following unitary definitions to each term

$$\begin{aligned}
R \propto C_{00} \frac{\sum_{k=1}^{n_r}(1 - P_{FA,k})P(H_{0,k}) \sum_{k=1}^{n_r} P(H_{0,k})}{\sum_{k=1}^{n_r} P(H_{0,k})} \\
+ C_{01} \frac{\sum_{k=1}^{n_r}(1 - P_{D,k})P(H_{1,k}) \sum_{k=1}^{n_r} P(H_{1,k})}{\sum_{k=1}^{n_r} P(H_{1,k})} \\
+ C_{10} \frac{\sum_{k=1}^{n_r} P_{FA,k}P(H_{0,k}) \sum_{k=1}^{n_r} P(H_{0,k})}{\sum_{k=1}^{n_r} P(H_{0,k})} \\
+ C_{11} \frac{\sum_{k=1}^{n_r} P_{D,k}P(H_{1,k}) \sum_{k=1}^{n_r} P(H_{1,k})}{\sum_{k=1}^{n_r} P(H_{1,k})}
\end{aligned} \tag{28}$$

and defining

$$P_{D_B} = \frac{\sum_{k=1}^{n_r} P_{D,k} P(H_{1,k})}{\sum_{k=1}^{n_r} P(H_{1,k})}$$
$$P_{FA_B} = \frac{\sum_{k=1}^{n_r} P_{FA,k} P(H_{0,k})}{\sum_{k=1}^{n_r} P(H_{0,k})} \quad (29)$$

then Eq. (28) can be written as

$$R \propto C_{00} \sum_{k=1}^{n_r} (1 - P_{FA_B}) P(H_{0,k}) + C_{01} \sum_{k=1}^{n_r} (1 - P_{D_B}) P(H_{1,k}) + C_{10} \sum_{k=1}^{n_r} P_{FA_B} P(H_{0,k}) + C_{11} \sum_{k=1}^{n_r} P_{D_B} P(H_{1,k}) \quad (30)$$

The term $P_{D_B}$ in Eq. (30), the Bayes probability of detection, is the expected proportion of the structure's damaged region correctly classified or, equivalently, the portion of the structure that exhibits the type II error. The term $P_{FA_B}$, the Bayes probability of false alarm, is the expected proportion of the structure's undamaged regions incorrectly classified or portion of the structure exhibiting type I error.

Finally, if one includes the cost of the system (including the SHM hardware deployment/maintenance costs, etc.) in the Bayes risk, $C_S$, the final form of Bayes risk/cost ($C_B$) takes the following form:

$$C_B = C_S + \sum_{k=1}^{n_r} C_{00} (1 - P_{FA_B}) P(H_{0,k}) + \sum_{k=1}^{n_r} C_{01} (1 - P_{D_B}) P(H_{1,k}) + \sum_{k=1}^{n_r} C_{10} P_{FA_B} P(H_{0,k}) + \sum_{k=1}^{n_r} C_{11} P_{D_B} P(H_{1,k}) \quad (31)$$

### 3.3 Definition of the objective functions

Once $P_{D_{sys}}$ is defined, it can be exploited for sensor network optimization in a damage identification scenario. Since most SHM applications require a combination of classification performance and cost minimization for a cost-effective implementation, both metrics are considered simultaneously in the following formulation. This work focuses on a multi-objective optimization procedure, designing a sensor network that maximizes the system probability of detection and, at the same time, minimizes the Bayes risk. Considering the structure is divided in $n_r$ regions as introduced in Section 3.2, the two objective functions are defined as:

$$\begin{cases} y_1 = -P_{D_{sys}} \\ y_2 = C_s + \sum_{k=1}^{n_r} C_{00} (1 - P_{FA_B}) P(H_{0,k}) + C_{01} (1 - P_{D_B}) P(H_{1,k}) + C_{10} P_{FA_B} P(H_{0,k}) + C_{11} P_{D_B} P(H_{0,k}), \end{cases} \quad (32)$$

where the first objective function, $y_1$, aims to maximize the global probability of detection or classification performance (expressed as minimizing its negative, since $P_{D_{sys}}$>0), while $y_2$ aims to minimize the Bayes risk ($R$) or cost ($C_B$). The latter includes costs associated with incorrect decisions and the system's explicit cost, incorporating eventual prior knowledge about structure's areas more prone to damage.

The cost-related parameters must be chosen according to the specific application and allow considering the entire SHM system life cycle in the design process. The remaining parameters $P(H_{0,k})$ and $P(H_{1,k})$ permit

one to include prior knowledge about the probability that region $k$ may be damaged or undamaged. The latter becomes particularly important when installing many sensors is impractical either from economic or technological points of view, possibly biasing sensors placement toward more critical areas. However, it is worth remarking that prior knowledge is not a mandatory input.

Since multi-objective optimizations likely return a family of solutions rather than a single one, a decision metric is defined. Considering a weighting parameter $\alpha$ governing the relative importance of the two objective functions, the optimal design, $d_{\mathrm{opt}}$, is considered as the sensor network minimizing the following relation:

$$d_{\mathrm{opt}} = \mathrm{argmin}_{\mathrm{d}}(\alpha y_1^2 + (1-\alpha) y_2^2) \tag{33}$$

Normalization of the two objective functions is desired before implementing Eq. (33), especially if they feature different signs or order of magnitude, to avoid wrong consideration of one of the two. A normalization between 0 and 1 as in Eq. (34) can be considered to implement Eq. (33).

$$\begin{cases} y_1 = \dfrac{y_1 - y_{1_{min}}}{y_{1_{max}} - y_{1_{min}}} \\ y_2 = \dfrac{y_2 - y_{2_{min}}}{y_{2_{max}} - y_{2_{min}}} \end{cases} \tag{34}$$

Once the optimal designs, $d_{\mathrm{opt}}$, are available as a function of the $\alpha$ coefficient, the designer can choose the best for the specific application. Applications demanding life-safety consideration might favor maximum classification/detection performance design (e.g., commercial airframe inspections), thus greater $\alpha$, while applications requiring minimized downtime (e.g., a manufacturing process) might favor a minimal risk/cost design (lower $\alpha$).

As a conclusion to Section 3, the primary workflow for implementing this multi-objective optimization strategy is shown in Fig. 3.

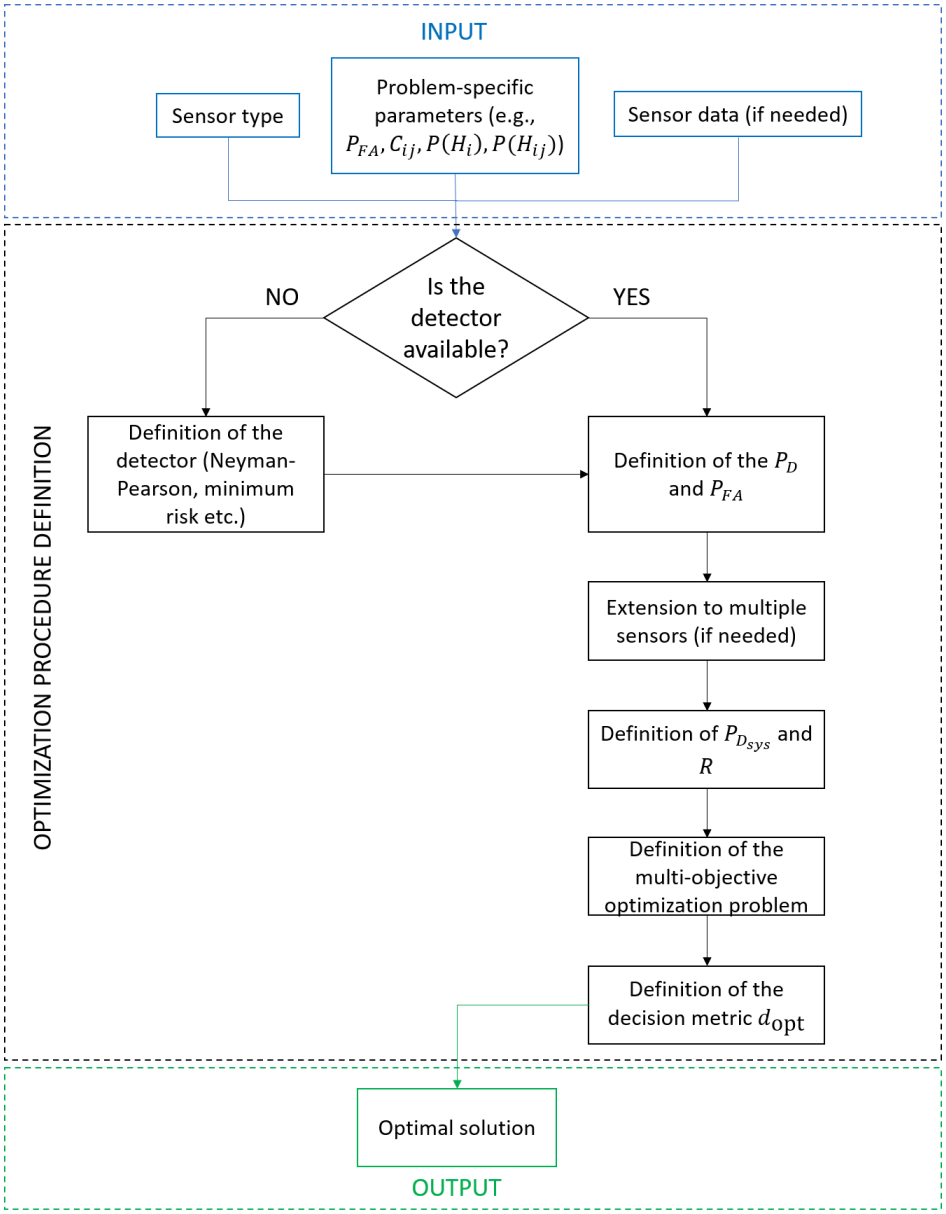


**Fig. 3. Flowchart of the methodology.**

## 4 The case study

The sensor network design through multi-objective optimization is presented with a cracked plate and a strain-based feature for damage identification. The reference specimen and the simulated strain measures are briefly described in this Section.

### 4.1 The specimen

The multi-objective optimization procedure for damage identification sensor network design is tested on a clamped plate with different crack damages. The plate has a length of $150\ mm$, a width of $60\ mm$, and a thickness of $5\ mm$, as shown in Fig. 4a.

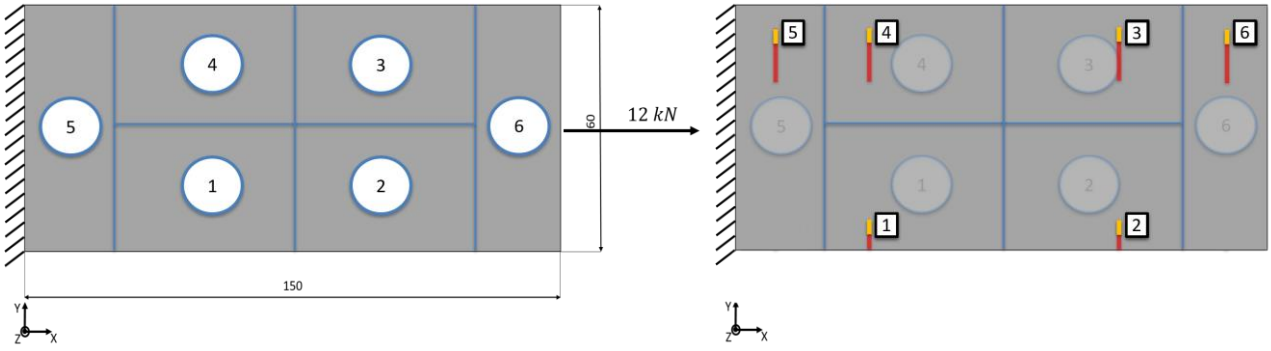


(a) (b)

**Fig. 4. The specimen and the damages; (a) The specimen with damage regions; (b) Graphical representation of the smallest (yellow) and biggest (red) simulated crack positions.**

The plate is made of Aluminum with an elastic modulus of $79\ GPa$ and a Poisson's ratio of 0.33. A load in the positive X direction with a magnitude of $12\ kN$ is applied at the specimen free end, simulating plate tension.

Six damage regions are considered in the specimen (Fig. 4a), and damages of different sizes are simulated within each area. Specifically, suppose that six damage positions are contemplated in the areas more prone to damaging with sizes spanning from $2.5\ mm$ to $15\ mm$ with steps of $2.5\ mm$ in positions 3-5 and from $2.5\ mm$ to $10\ mm$ in positions 1-2, as shown in Fig. 4b. This discretization considers different types of cracks, investigating the method's ability to cope with non-homogenous damages.

### 4.2 The direct FEM for strain measure simulation

The index ($i(t)$) for damage identification is derived comparing strains in the actual condition ($A(t)$) to a reference baseline ($B$), reflected in an index deviation from the null condition if the structure is damaged. The pattern of strain measures is numerically simulated with a Finite Element Model (FEM) of the plate. The latter is generated in ABAQUS with a high-fidelity mesh consisting of 9000 S4 shell elements. Fatigue crack damage is implemented using the SEAM function available in ABAQUS, thus duplicating the nodes along the crack edge for crack opening when the specimen is loaded.

The FE model is used to generate strain patterns in healthy and damaged states, followed by evaluating the different method responses when the numerically simulated strain measures are considered for computing the probability of detection. An example of the strain pattern and the deformed configuration simulated for different crack positions and sizes is shown in Fig. 5, visualizing the influence of different damages on the strain field. Numerical noise, modeled as white Gaussian noise with a standard deviation $\sigma_X = 5\ \mu\varepsilon$ is added to the baseline and actual measures, enabling the implementation of a statistical hypothesis testing as in Eqs. (2) and (3). The standard deviation value is chosen to simulate realistic performances of strain's acquisition systems.

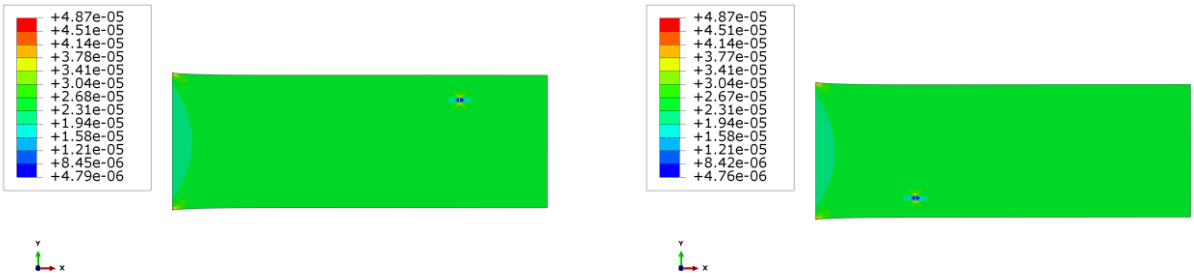


(a) (b)

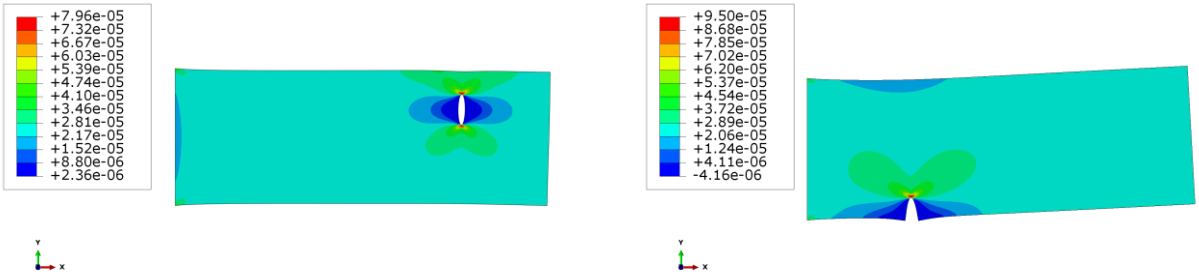


(c) (d)

**Fig. 5. Example of strain fields ($\varepsilon_{xx}$) due to cracks; (a) 2.5 mm crack in position 3; (b) 2.5 mm crack in position 1; (c) 15 mm crack in position 3; (d) 10 mm crack in position 1.**

## 5. Results

The optimization is carried out with a genetic algorithm for its well-established robustness. It is not the authors intention to enter into the details of related theory background, while the interested reader can refer to [42] for review.

The optimal sensor placement results are presented in this Section for the case study in Section 4. Firstly, the procedure is presented for a reference set of cost parameters (Section 5.1) and compared to engineering solutions (Section 5.2). A sensitivity analysis of the Bayes risk's parameters is performed, providing insights into their influence on the network. Solutions obtained with a multi-objective framework are compared to single-objective optimal designs in Section 5.4, and, finally, the Receiver Operating Characteristic (ROC) curves are shown for different optimal networks in Section 5.5.

### 5.1 The reference sensor network design

The optimal design solution is a function of the parameters in Eq. (32) that are set according to the specific application. The parameters are defined as a function of the costs of normal operation ($C_{00}$) and are summarized in Table 1. Since the strain values do not feature a considerable gradient, the simulated measures are extracted considering a coarser grid of sensors with $5\ mm$ spacing to reduce the computational time. Thus, a maximum of 360 sensors can potentially be installed on the plate.

| Parameter | Value | Parameter | Value |
|---|---|---|---|
| $C_{00}$ | $1$ | $P(H_1)$ | $0.5$ |
| $C_{10}$ | $100C_{00}$ | $P(H_0)$ | $0.5$ |
| $C_{01}$ | $10^4C_{00}$ | $P(H_{0,k})$ | $1.4 \cdot 10^{-3}$ |
| $C_{11}$ | $300C_{00}$ | $P(H_{1,k})$ | $1.4 \cdot 10^{-3}$ |
| $C_s$ | $2C_{00} \cdot n_s$ | $P_{FA}$ | $10^{-3}$ |

**Table 1. Cost parameters summary.**

Subplots of Fig. 6 show the optimal design results. The optimal design front, $d_{\text{opt}}$, according to Eq. (33), is highlighted in Fig. 6a with red dots as a function of different $\alpha$ values. Notice that proper normalizations between 0 and 1 of the two objective functions as in Eq. (34) are performed before computing the decision metric to consider the two functions properly. The two extreme values for $\alpha$ in Eq. (33), i.e., $\alpha = 0$ and $\alpha = 1$, bias the multi-objective function toward a single target for the optimal design. Specifically, $\alpha = 0$ considers only the minimum Bayes cost in the Pareto front solutions, favoring solutions with a lower cost of the system and, thus, fewer sensors (Fig. 6b). On the other hand, $\alpha = 1$ means that maximization of the health classification performances is chosen for optimal decision criterium, and solutions tending to saturate all the sensor positions available are promoted (Fig. 6d). The relative importance of the two objective functions varies with $\alpha$, and one can choose the best approach for the specific application. Values of $\alpha$ closer to 0 tend to solutions favoring cost reduction, while values closer to 1, solutions that maximize detection probability. A value of $\alpha = 0.5$ (Fig. 6c) considers a perfect balance between the functions, being the design solution

closest to the Utopia point [43], which ideally minimizes both functions simultaneously. It is worth remarking that the Utopia point does not exist for non-trivial multi-objective optimization problems.

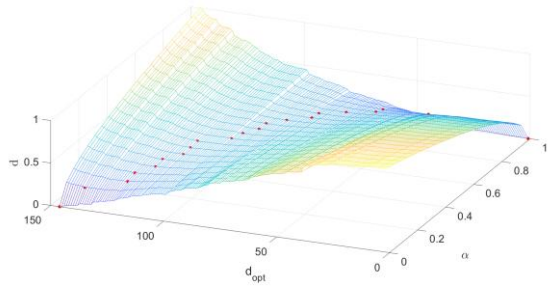


(a)

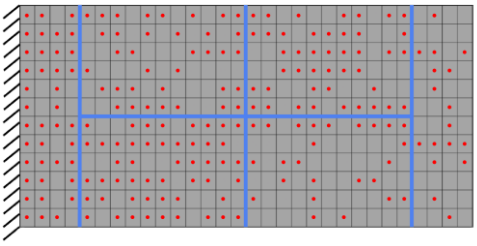

(b) $\alpha = 0$

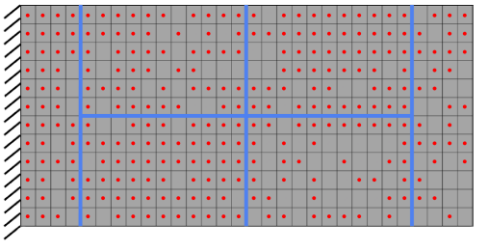

(c) $\alpha = 0.5$

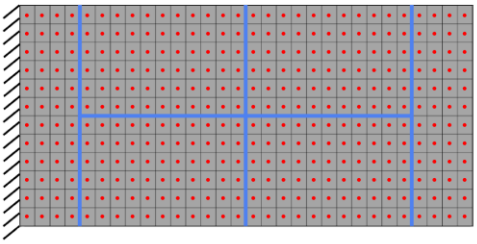

(d) $\alpha = 1$

**Fig. 6. The optimal sensor design; (a) The optimal design choice (red circles) as a function of $\alpha$; (b) The optimal sensor network ($\alpha$=0); (c) The optimal sensor network ($\alpha$=0.5); (d) The optimal sensor network ($\alpha$=1).**

### 5.2 Comparison with engineering solutions

Whenever an optimization problem is involved, it is worth investigating if the optimized solution outperforms easier and less demanding designs that one can obtain with simple engineering judgment. The optimal design solutions of Section 5.1 are compared with many sensor networks, differently covering the plate area in a structured way and reflecting the uniform prior probability of damage, $P(H_{1,k}) = c$ (with $c$ a constant value), in each region. Different solutions have been tested; however, only four networks with an increasing number of sensors are reported for brevity in this section. Fig. 7 shows the structured solutions aiming at the best geometrical plate coverage for different sensor numbers to consider varying SHM system costs in the Bayes risk objective function.

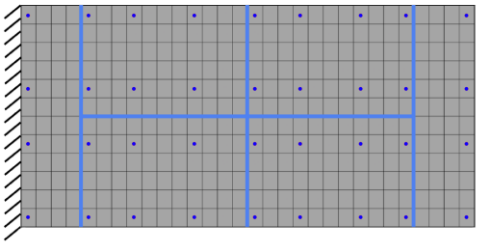

(a) Structured 1

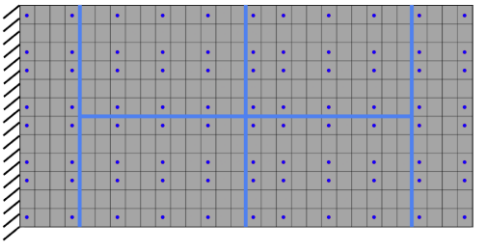

(b) Structured 2

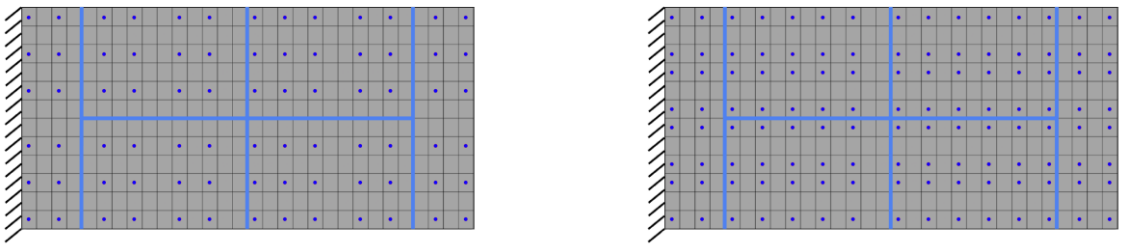

(c) Structured 3 (d) Structured 4

**Fig. 7. The structured engineering designs.**

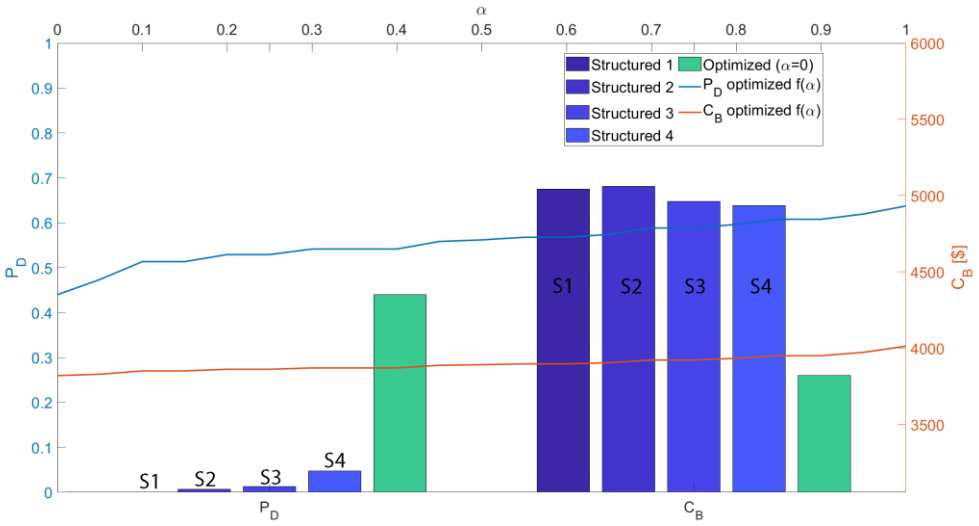


**Fig. 8. Comparison of the probability of detection and Bayes cost between optimized and engineering solutions.**

The solutions are compared in terms of damage classification capability ($P_D$) and cost ($C_B$). Fig. 8 highlights the results separately for each testing metric. Blue bars refer to the different structured designs in Fig. 7, while the green bar to the optimal design solution for $\alpha = 0$. One can notice that the optimal design outperforms all the structured solutions in terms of costs and classification performances. An increase of about 816% compared to the best structured option (0.440 vs. 0.048) is achieved in the detection capability with a cost reduction of 23%, proving the additional optimization work is justified. Furthermore, the red and blue lines represent the probability of detections and Bayes costs as a function of $\alpha$. Useful information from a decisional point of view can be extracted from the graph. One can readily compare the cost of performance variations as a function of the two metrics' relative importance. Indeed, the $\alpha = 0.6$ design features a classification improvement of 29%, passing from $0.440$ ($\alpha = 0$) to $0.568$ ($\alpha = 0.6$), with a small supplement of cost (3821 $ vs. 3898 $, about +2%). The improvement of classification relative to the cost increase can be evaluated with a synthetic index, $CtoC = \frac{\frac{P_D(\alpha)}{P_D(\alpha=0)}-1}{\frac{C_B(\alpha)}{C_B(\alpha=0)}-1}$. Fig. 9 shows the index as a function of $\alpha$. The design for $\alpha = 0.05$ features the biggest classification improvement for the smallest increase in the cost (+31), resulting in the design configuration pursuing the highest increase of probability of detection with the minimum increase in Bayes cost.

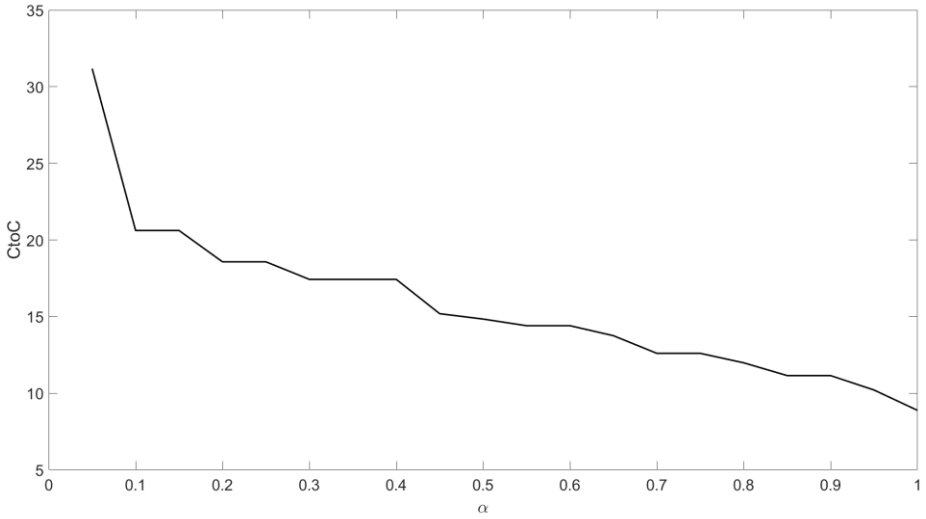


**Fig. 9. Classification improvement to cost increase ratio as a function of $\alpha$.**

### 5.3 Sensitivity analysis on the cost parameters

The optimization results are strongly influenced by the parameters included in the Bayes cost definition. In this section, a sensitivity analysis on the cost parameters is performed to understand each parameter's relative influence on the results. Specifically, Fig. 10 and Fig. 11 show the results for varying parameters and prior probabilities of damage in the structure.

Optimal designs like in Section 5.1 are obtained for varying costs of correct decisions, $C_{11}$, and in the limit condition where only the costs of wrong decisions are considered. A negligible effect on the results is also produced for varying false positives costs, with almost unaffected solutions when the parameter is decreased by one order of magnitude. The same solution that maximizes the probability of detection is obtained for all the parameter combinations when $\alpha = 1$. If $\alpha$=1, only the first objective function is considered in the decision metric, and the solutions are unaffected by the cost parameters variations. Two parameters mostly impact the results, i.e., $C_s$ and $C_{01}$. Increasing the system's cost or reducing the false negatives' cost, the optimization favors designs with fewer sensors. The latter is due to a more significant impact of additional sensors on the cost, if $C_s$ is increased, and relaxation on the consequences for missed damages for reduced cost of false negatives. It is interesting noticing the algorithm behavior in the limiting condition of a negligible cost of the system ($C_s = 0$) or too high cost of false alarms (Fig. 10a). When one of the previously described conditions is met, the optimization degenerates in a trivial multi-objective optimization, and all the Pareto front solutions collapse in the Utopia point. The two objective functions become comparable, and a unique solution is found for the multi-objective problem.

Fig. 11 shows the influence of different prior probabilities of damage on the sensor networks. The influence of different prior damage probabilities within the plate are investigated, considering small variation compared to the uniform distribution (e.g., Fig. 11a) up to prior probabilities completely biased toward one region (e.g., Fig. 11l). Prior knowledge in the optimization procedure can favor solution designs exploiting information from previous experiments. The latter is crucial if the number of sensors is constrained and previous experience evidenced areas more prone to damage. Even though results mostly reflect prior knowledge (e.g., Fig. 11b or Fig. 11h), the algorithm does not blindly mirror the prior probability distribution. The latter is particularly visible in Fig. 11m, where, despite a prior probability completely biased toward Region 1 (Fig. 11l), the sensors are not installed only in that region. Indeed, the probability of detection is computed with damages simulated in all the regions, inducing sensor placement in Region 2-6 even though in a smaller quantity compared to Region 1, demonstrating that the method can also cope with wrong prior information.

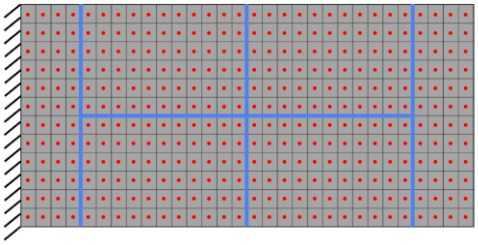

(a) $C_s = 0$ or $C_{01} = 10^7$ or $\alpha = 1$

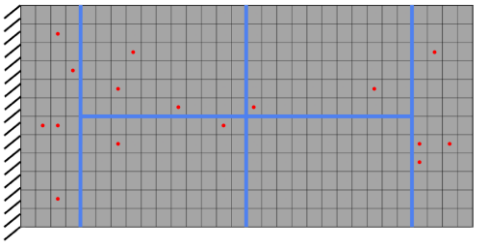

(b) $C_{01} = 10^3 \ \ (\alpha = 0)$

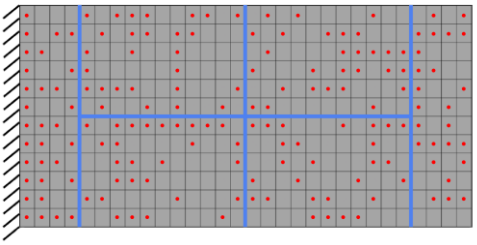

(c) $C_{01} = 10^3 \ \ (\alpha = 0.5)$

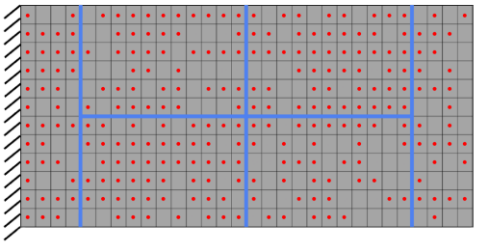

(d) $C_{10} = 10 \ \ (\alpha = 0)$

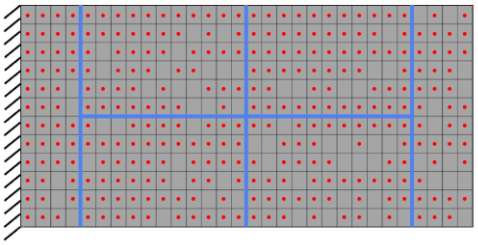

(e) $C_{10} = 10 \ \ (\alpha = 0.5)$

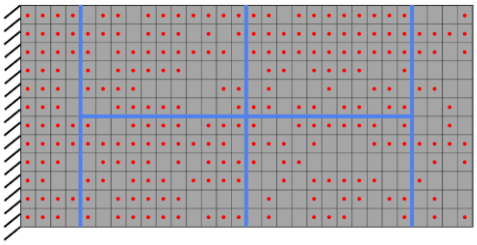

(f) $C_{11} = 600 \ \ (\alpha = 0)$

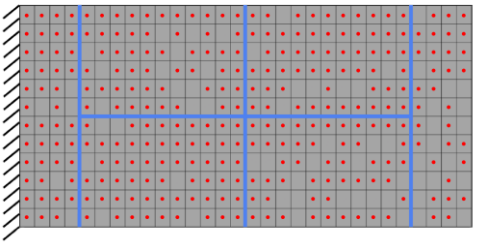

(g) $C_{11} = 600 \ \ (\alpha = 0.5)$

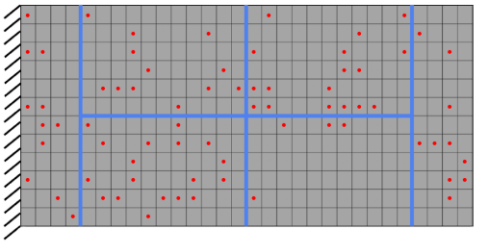

(h) $C_s = 10 \ \ (\alpha = 0)$

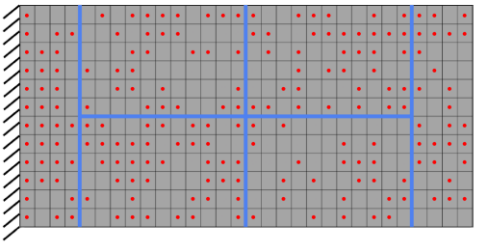

(i) $C_s = 10 \ \ (\alpha = 0.5)$

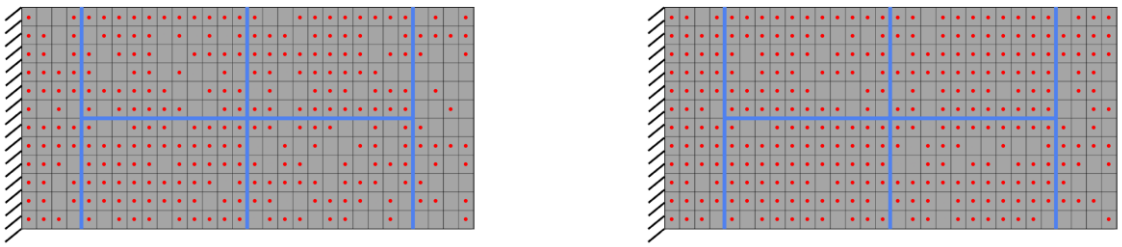

(l) $C_{00} = C_{11} = 0$ $(\alpha = 0)$ (m) $C_{00} = C_{11} = 0$ $(\alpha = 0.5)$

**Fig. 10. Sensor design for different cost parameters and $\alpha$.**

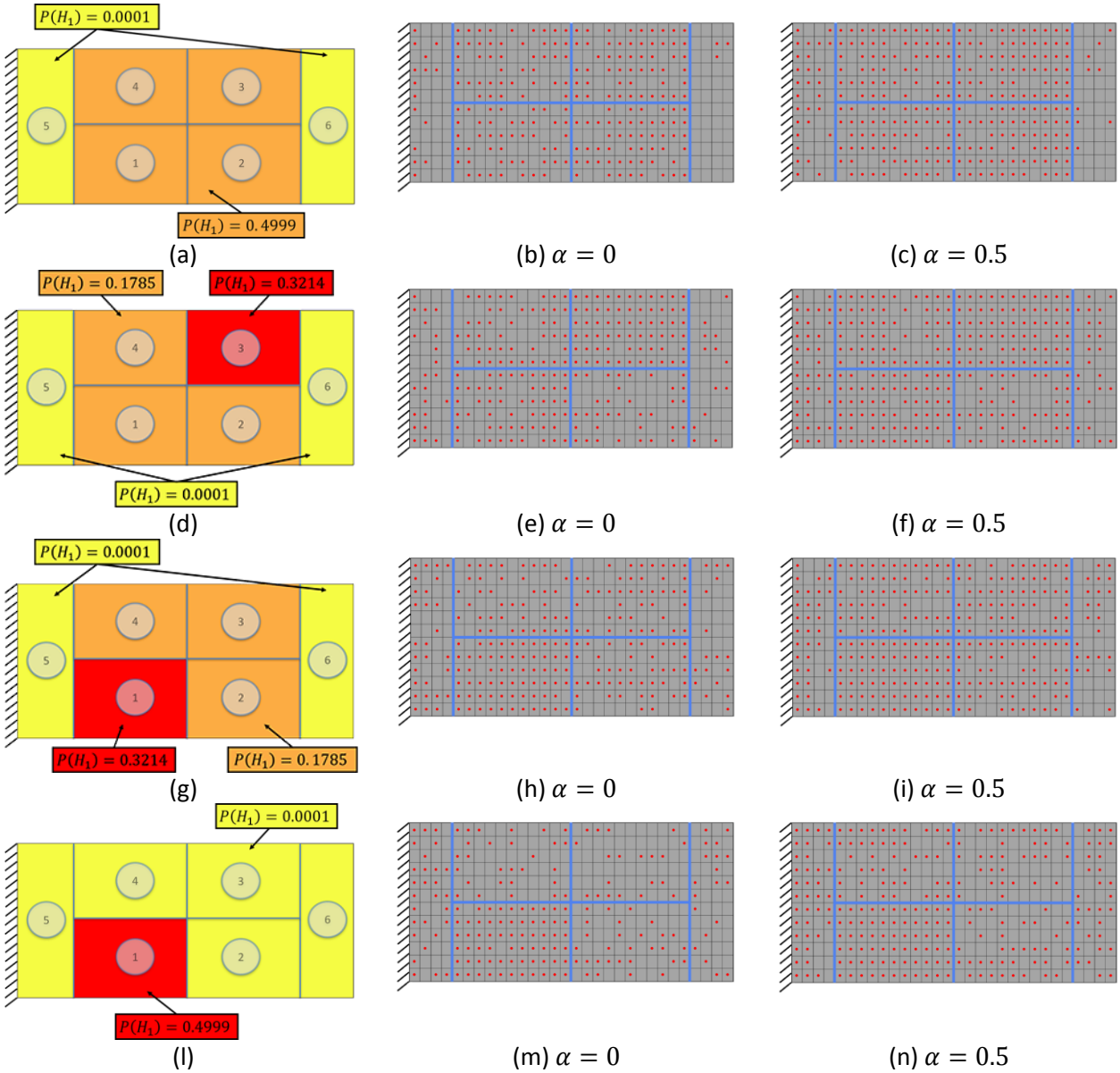


(a) (b) $\alpha = 0$ (c) $\alpha = 0.5$

(d) (e) $\alpha = 0$ (f) $\alpha = 0.5$

(g) (h) $\alpha = 0$ (i) $\alpha = 0.5$

(l) (m) $\alpha = 0$ (n) $\alpha = 0.5$

**Fig. 11. Optimal designs ($\alpha = 0$ and $\alpha = 0.5$) with different prior probabilities of damage (left column).**

### 5.4 Comparison between single and multi-objective optimizations

In this work, the sensor placement strategy is based on multi-objective optimization. However, usually, one either maximizes the classification performance or minimizes the cost, without considering how the choice of one optimization logic affects other's metrics. In this section, the single objective minimization of the cost is compared with the corresponding multi-objective solution ($\alpha = 0$). The two optimizations feature a $C_s = 10$ to further highlights the differences in the solutions of the two approaches. Notice that the comparison between the single-objective solution maximizing the probability of damage and the corresponding multi-objective design ($\alpha = 1$) degenerates in the same solution, as described in Section 5.3, and for this reason is not reported.

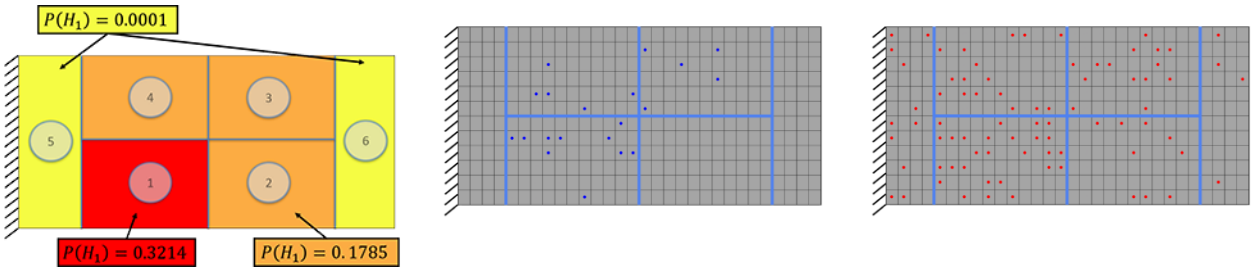


(a) (b) Single-objective (Bayes cost) (c) Multi-objective ($\alpha = 0$)

**Fig. 12. Single and multi-objective optimal designs with a non-uniform prior probability of damage and $C_s = 10$.**

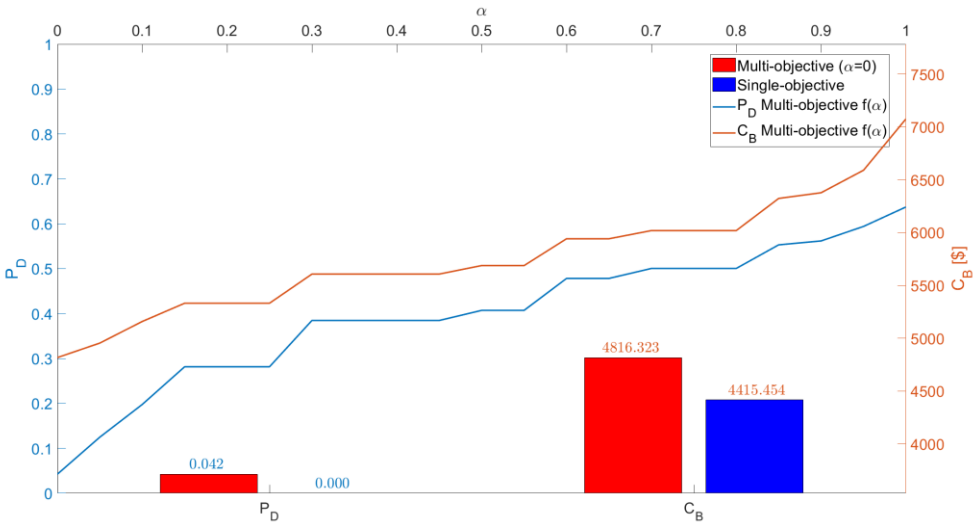


**Fig. 13. Multi and single-objective solutions performances in terms of Bayes cost and probability of detection.**

The two solutions are shown in Fig. 12 with a non-uniform prior probability of damage, as in Fig. 12a. One can readily notice that the single-objective optimization design solution features a lower number of sensors compared to the multi-objective design considering only the Bayes-cost in the decision metric $d_{\text{opt}}$. The latter is due to the influence of the Neyman-Pearson objective function in the Pareto front of the multi-objective optimization even when only the Bayes cost is considered in $d_{\text{opt}}$. Indeed, the metric is computed from the Pareto front, where the two objective functions influence each other. The impact of the first objective function in the results is even more evident in Fig. 13, where the values of the Bayes cost ($C_B$) and probability of detection ($P_D$) are compared. The cost increment of the multi-objective design ($+9\%$) is highly compensated by a system probability of detection order of magnitudes greater than the single-objective one. The gap can be further increased if one considers the design solution for $\alpha = 0.05$, which possesses a $P_D$ about 3 times bigger than for $\alpha = 0$, with an increase in the cost of only 3%.

### 5.5 The Receiver Operating Characteristic (ROC) curves

The previous sections' results are obtained with a fixed probability of false alarms, $P_{FA}$, when computing the threshold for damage classification, $\gamma'$. However, the system performance in terms of probability of detection is usually provided as a function of the probability of false alarms, possibly defining the Receiver Operating Characteristic (ROC) curves.

The optimal design solutions ($\alpha = 0$) as a function of the probability of detection are visually compared in Fig. 14, considering a biased prior probability of damage. The effect of relaxing the constraint on the admissible false alarm rate in the health classification threshold is promptly visible. Sensor networks with fewer sensors are favored for increasing $P_{FA}$. Indeed, a threshold associated with a higher false allowance rate returns a detector with a higher probability of detection and, consequently, the same effect can be obtained in the objective functions with a lower number of sensors.

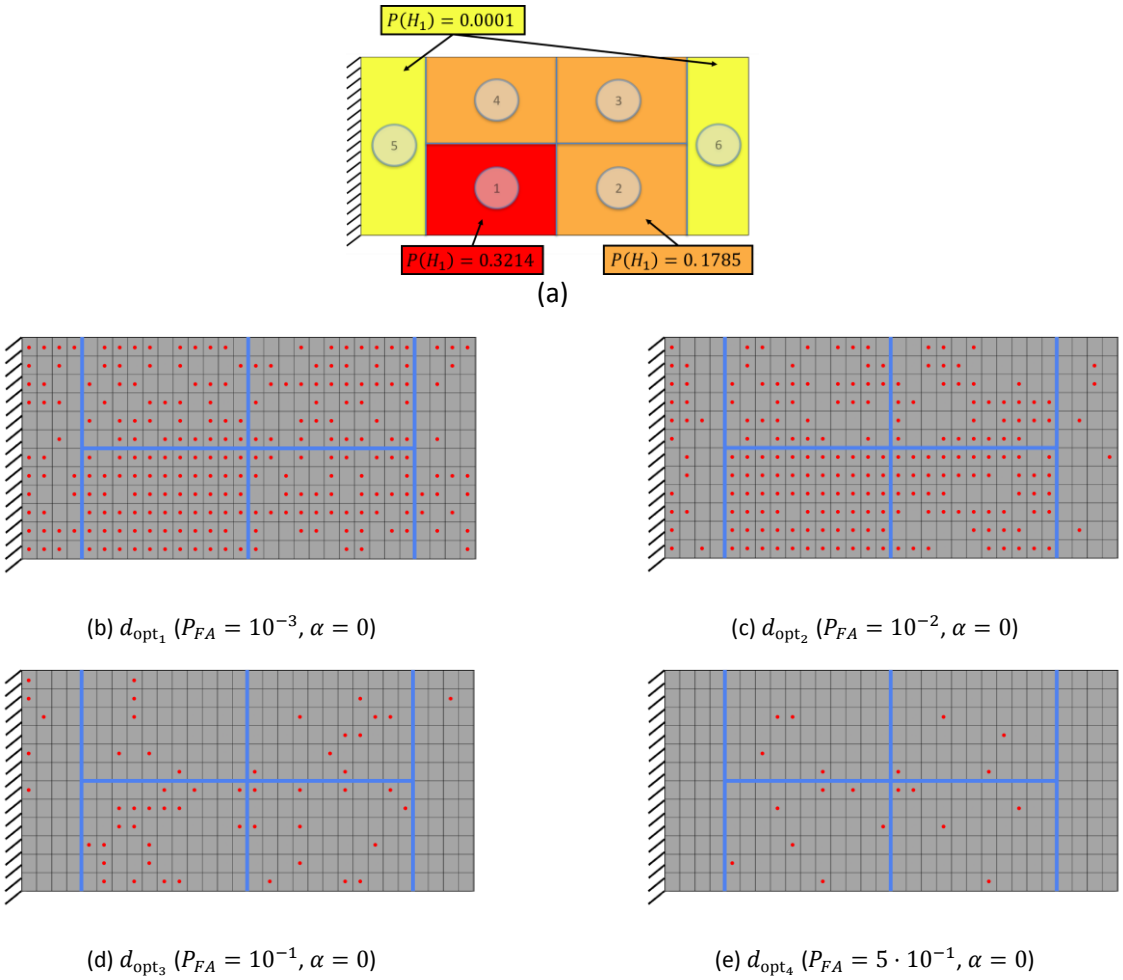


(a)

(b) $d_{\text{opt}_1}$ ($P_{FA} = 10^{-3}$, $\alpha = 0$)

(c) $d_{\text{opt}_2}$ ($P_{FA} = 10^{-2}$, $\alpha = 0$)

(d) $d_{\text{opt}_3}$ ($P_{FA} = 10^{-1}$, $\alpha = 0$)

(e) $d_{\text{opt}_4}$ ($P_{FA} = 5 \cdot 10^{-1}$, $\alpha = 0$)

**Fig. 14. Optimal designs for different probability of false alarms.**

The same four optimal sensor network designs are used to compute the ROC curves of the SHM system. Fig. 15 shows the probability of detection for each $d_{\text{opt}}$ as a function of the parameters $\alpha$ and $P_{FA}$. As expected, the performances in terms of $P_D$ differ mostly for low $\alpha$ or $P_{FA}$, while tending to similar performances for relatively high $P_{FA}$ (Fig. 15a). The ROC curves for $\alpha = 0$ are shown in Fig. 15b. The converging behavior is visible for optimal designs $d_{\text{opt}_1} - d_{\text{opt}_3}$ and $P_{FA} > 0.05$. However, $d_{\text{opt}_4}$ features the slowest converging rate since the number of sensors is the lowest. The convergence rate is higher if considering $\alpha$ tending to 1 (Fig. 15a). Finally, the ROC curves are shown for fixed $P_{FA} = 10^{-3}$ (Fig. 15c), as in the previous sections, and providing the corresponding Bayes cost, normalized between 0 and 1, for each point of the curve and computed for $P_{FA} = 10^{-3}$. Generally, the Bayes cost increases as the optimal designs with higher false

allowance are considered. The lowest costs are, indeed, found for $d_{\mathrm{opt}_1}$. The ROC curves are computed for $P_{FA} = 10^{-3}$, which is also the probability of false alarm considered while optimizing $d_{\mathrm{opt}_1}$. Thus, the solution behaves better in terms of Bayes costs and probability of detections, confirming the design behaves optimally for the specific conditions.

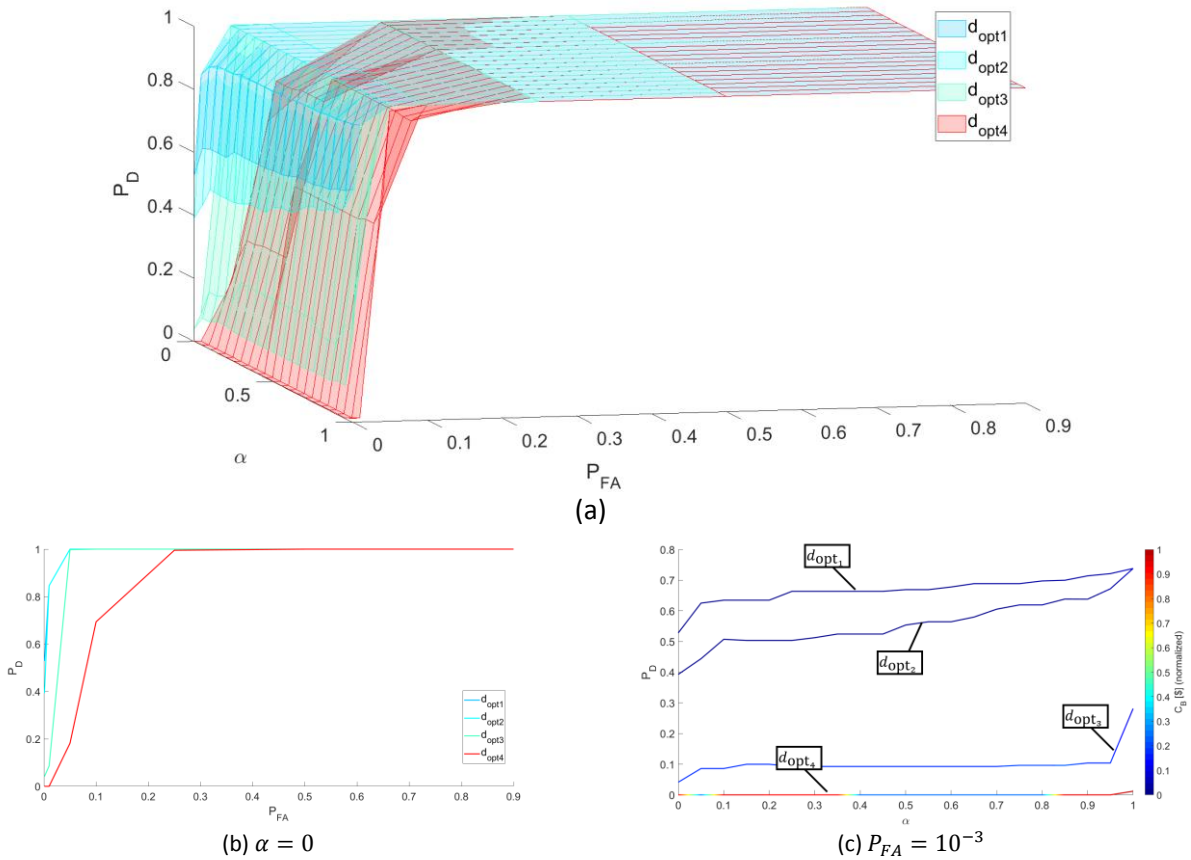


**Fig. 15. ROC curves; (a) ROC curves for different alpha; (b) ROC curves ($\alpha = 0$); (b) ROC curves and Bayes costs for $P_{FA} = 10^{-3}$.**

## 6. Conclusions

A rigorous unified and consistent framework for optimal statistical detector definition and sensor placement is described in this work. An optimal statistical detector for anomaly detection is defined based on the Neyman-Pearson likelihood ratio test and is exploited in a multi-objective optimization paradigm for SHM sensor network design. The results detailed in this work are thoroughly documented to provide the reader with a critical method for interpreting multi-objective optimization results and systematically produce optimal sensor networks for SHM.

The optimal statistical detector is constructed for typical SHM damage sensitive features based on a squared difference between the actual and reference conditions. The detector performance in terms of classification is then exploited for multi-objective optimization of an SHM sensor network. The optimization aims to balance maximization of the classification performances and minimization of the total cost (or Bayes risk). The latter is a function of different costs, including type I and II decision error costs and the SHM system cost. However, it usually provides a contrasting solution design compared to a maximum detection approach, despite being both fundamental aspects for an industrially-competitive SHM system.

Numerical results with a cracked plate show the method attractiveness for designing data collection systems systematically. The optimal strain-based sensing design features significant improvements in cost reduction

and performance enhancements than networks defined based on engineering judgement only. Different sensitivity analyses have been performed, investigating the Bayes cost parameters influence on the results, and detailing the most significant one. Furthermore, the multi-objective optimal designs have been compared with single-objective ones, illustrating the main difference between the two and demonstrating an overall better performance in the detection efficiency over cost. The Receiver Operating Characteristic (ROC) curves are also provided as a function of different designs.

Finally, even though not reported here, the optimal detector construction and the sensor placement design remain valid with different damage-sensitive features and sensor types, e.g., an ultrasonic distributed monitoring system based on piezoelectric sensors. The only thing that changes is the specific measurement model process that leads to the specific formulation of the various probability terms. The authors' future research will be devoted to implementing the method with different SHM scenarios and algorithms extremely sensitive to proper sensor network definition.

**Bibliography**


[1] L. Colombo, C. Sbarufatti, and M. Giglio, "Definition of a load adaptive baseline by inverse finite element method for structural damage identification," *Mech. Syst. Signal Process.*, vol. 120, pp. 584–607, 2019.

[2] C. Bigoni and J. S. Hesthaven, "Simulation-based Anomaly Detection and Damage Localization: an application to Structural Health Monitoring," *Comput. Methods Appl. Mech. Eng.*, vol. 363, 2020.

[3] I. Benedetti, M. H. Aliabadi, and A. Milazzo, "A fast BEM for the analysis of damaged structures with bonded piezoelectric sensors," *Comput. Methods Appl. Mech. Eng.*, vol. 199, no. 9–12, pp. 490–501, 2010.

[4] H. Guo and L. Zhang, "A weighted balance evidence theory for structural multiple damage localization," *Comput. Methods Appl. Mech. Eng.*, vol. 195, no. 44–47, pp. 6225–6238, 2006.

[5] P. Seventekidis, D. Giagopoulos, A. Arailopoulos, and O. Markogiannaki, "Structural Health Monitoring using deep learning with optimal finite element model generated data," *Mech. Syst. Signal Process.*, vol. 145, p. 106972, 2020.

[6] C. R. Farrar and K. Worden, "An introduction to structural health monitoring," *Philos. Trans. R. Soc. A Math. Phys. Eng. Sci.*, vol. 365, no. 1851, pp. 303–315, 2007.

[7] T.-H. Yi, H.-N. Li, and M. Gu, "Optimal sensor placement for structural health monitoring based on multiple optimization strategies," *Struct. Des. Tall Spec. Build.*, vol. 20, no. 7, pp. 881–900, 2011.

[8] T.-H. Yi, X.-J. Yao, C.-X. Qu, and H.-N. Li, "Clustering number determination for sparse component analysis during output-only modal identification," *J. Eng. Mech.*, vol. 145, no. 1, 2019.

[9] T.-H. Yi, H.-N. Li, and X.-D. Zhang, "A modified monkey algorithm for optimal sensor placement in structural health monitoring," *Smart Mater. Struct.*, vol. 21, no. 10, 2012.

[10] H. W. Park, H. Sohn, K. H. Law, and C. R. Farrar, "Time reversal active sensing for health monitoring of a composite plate," *J. Sound Vib.*, vol. 302, no. 1–2, pp. 50–66, 2007.

[11] S. R. Anton, G. Park, C. R. Farrar, and D. J. Inman, "On piezoelectric Lamb wave-based structural health monitoring using instantaneous baseline measurements," in *Proceedings of SPIE - The International Society for Optical Engineering*, 2007, vol. 6532.

[12] L. Colombo, D. Oboe, C. Sbarufatti, F. Cadini, S. Russo, and M. Giglio, "Shape sensing and damage

identification with iFEM on a composite structure subjected to impact damage and non-trivial boundary conditions," *Mech. Syst. Signal Process.*, vol. 148, p. 107163, 2021.

[13] C. Argyris, S. Chowdhury, V. Zabel, and C. Papadimitriou, "Bayesian optimal sensor placement for crack identification in structures using strain measurements," *Struct. Control Heal. Monit.*, vol. 25, no. 5, 2018.

[14] W. A. Maul, G. Kopasakis, L. M. Santi, T. S. Sowers, and A. Chicatelli, "Sensor selection and optimization for health assessment of aerospace systems," *J. Aerosp. Comput. Inf. Commun.*, vol. 5, no. 1, pp. 16–24, 2008.

[15] E. B. Flynn and M. D. Todd, "An active sensor placement optimization strategy using Bayesian experimental design," in *Bridge Maintenance, Safety, Management and Life-Cycle Optimization - Proceedings of the 5th International Conference on Bridge Maintenance, Safety and Management*, 2010, pp. 173–179.

[16] C. Yang, K. Liang, and X. Zhang, "Strategy for sensor number determination and placement optimization with incomplete information based on interval possibility model and clustering avoidance distribution index," *Comput. Methods Appl. Mech. Eng.*, vol. 366, 2020.

[17] S. Cantero-Chinchilla, J. Chiachío, M. Chiachío, D. Chronopoulos, and A. Jones, "Optimal sensor configuration for ultrasonic guided-wave inspection based on value of information," *Mech. Syst. Signal Process.*, vol. 135, p. 106377, 2020.

[18] V. Giurgiutiu, A. Zagrai, and J. J. Bao, "Piezoelectric wafer embedded active sensors for aging aircraft structural health monitoring," *Struct. Heal. Monit.*, vol. 1, no. 1, pp. 41–61, 2002.

[19] D. C. Kammer, "Sensor placement for on-orbit modal identification and correlation of large space structures," *J. Guid. Control. Dyn.*, vol. 14, no. 2, pp. 251–259, 1991.

[20] M. Luong, D. Maquin, C. T. Huynh, and J. Ragot, "Observability, redundancy, reliability and integrated design of measurement systems," in *2nd IFAC Symposium on Intelligent Components and Instruments for Control Applications, SICICA'94*, 1994.

[21] A. Kretsovalis and R. S. H. Mah, "Observability and redundancy classification in generalized process networks-II. Algorithms," *Comput. Chem. Eng.*, vol. 12, no. 7, pp. 689–703, 1988.

[22] D. Dochain, N. Tali-Maamar, and J. P. Babary, "On modelling, monitoring and control of fixed bed bioreactors," *Comput. Chem. Eng.*, vol. 21, no. 11, pp. 1255–1266, 1997.

[23] C. Bigoni, Z. Zhang, and J. S. Hesthaven, "Systematic sensor placement for structural anomaly detection in the absence of damaged states," *Comput. Methods Appl. Mech. Eng.*, vol. 371, 2020.

[24] L. Colombo *et al.*, "Numerical and experimental verification of an inverse-direct approach for load and strain monitoring in aeronautical structures," *Struct. Control Heal. Monit.*, vol. 28, no. 2, 2021.

[25] M. Bagajewicz, A. Fuxman, and A. Uribe, "Instrumentation network design and upgrade for process monitoring and fault detection," *AIChE J.*, vol. 50, no. 8, pp. 1870–1880, 2004.

[26] R. Raghuraj, M. Bhushan, and R. Rengaswamy, "Locating sensors in complex chemical plants based on fault diagnostic observability criteria," *AIChE J.*, vol. 45, no. 2, pp. 310–322, 1999.

[27] M. Bhushan and R. Rengaswamy, "Design of sensor network based on the signed directed graph of the process for efficient fault diagnosis," *Ind. Eng. Chem. Res.*, vol. 39, no. 4, pp. 999–1019, 2000.

[28] S. Kolluri, I. Bajaj, and M. Bhushan, "Sensor network design for efficient fault diagnosis and signed digraph update," in *IFAC Proceedings Volumes (IFAC-PapersOnline)*, 2013, vol. 10, no. PART 1, pp. 821–826.

[29] E. B. Flynn and M. D. Todd, “Optimal placement of piezoelectric actuators and sensors for detecting damage in plate structures,” *J. Intell. Mater. Syst. Struct.*, vol. 21, no. 3, pp. 265–274, 2010.

[30] E. B. Flynn and M. D. Todd, “A Bayesian approach to optimal sensor placement for structural health monitoring with application to active sensing,” *Mech. Syst. Signal Process.*, vol. 24, no. 4, pp. 891–903, 2010.

[31] E. B. Flynn and M. D. Todd, “A Bayesian experimental design approach to structural health monitoring,” in *Proceedings of the 5th European Workshop - Structural Health Monitoring 2010*, 2010, pp. 414–419.

[32] E. B. Flynn and M. D. Todd, “Bayesian probabilistic structural modeling for optimal sensor placement in ultrasonic guided wave-based structural health monitoring,” in *Proceedings of SPIE - The International Society for Optical Engineering*, 2010, vol. 7648.

[33] G. Capellari, E. Chatzi, S. Mariani, and S. E. Azam, “Optimal design of sensor networks for damage detection,” in *Procedia Engineering*, 2017, vol. 199, pp. 1864–1869.

[34] G. Capellari, E. Chatzi, and S. Mariani, “An optimal sensor placement method for SHM based on Bayesian experimental design and Polynomial Chaos Expansion,” in *ECCOMAS Congress 2016 - Proceedings of the 7th European Congress on Computational Methods in Applied Sciences and Engineering*, 2016, vol. 3, pp. 6272–6282.

[35] G. Capellari, E. Chatzi, and S. Mariani, “Cost–benefit optimization of structural health monitoring sensor networks,” *Sensors (Switzerland)*, vol. 18, no. 7, 2018.

[36] S. M. Kay, *Fundamentals of Statistical Signal Processing: Detection theory*. Prentice-Hall PTR, 1998.

[37] T.-H. Yi, H.-N. Li, and M. Gu, “Optimal sensor placement for health monitoring of high-rise structure based on genetic algorithm,” *Math. Probl. Eng.*, vol. 2011, 2011.

[38] C. Papadimitriou, “Pareto optimal sensor locations for structural identification,” *Comput. Methods Appl. Mech. Eng.*, vol. 194, no. 12–16, pp. 1655–1673, 2005.

[39] D. J. Olive, *Statistical theory and inference*. Springer, 2014.

[40] S. R. Eliason, *Maximum likelihood estimation: Logic and practice*, no. 96. Sage, 1993.

[41] X. Wang, G. Foliente, Z. Su, and L. Ye, “Information Fusion in Distributed Sensor Network for Structural Damage Detection,” in *Composite Technologies for 2020*, L. Ye, Y.-W. Mai, and Z. Su, Eds. Woodhead Publishing, 2004, pp. 1005–1011.

[42] M. Mitchell, *An introduction to genetic algorithms*. MIT press, 1998.

[43] L. Lu, C. M. Anderson-Cook, and T. J. Robinson, “Optimization of designed experiments based on multiple criteria utilizing a Pareto frontier,” *Technometrics*, vol. 53, no. 4, pp. 353–365, 2011.